This preprint has undergone one round of review in *Earth and Planetary Science Letters* and has been accepted for publication (as of April 2024)

Persistent Geochemical Zonation ("Striping") within the Galápagos Mantle Plume

Matthew Gleeson[1]*, Mark Richards[1], Cinzia G. Farnetani[2], Kaj Hoernle[3], and Sally Gibson[4]

[1]Department of Earth and Planetary Science, University of California Berkeley, 94703, USA
[2]Université Paris Cité et Institut de Physique du Globe, Paris, France
[3]GEOMAR Helmholtz Centre for Ocean Research Kiel, Kiel, Germany
[4]Department of Earth Sciences, University of Cambridge, CB1 1JU, UK

*gleesonm@berkeley.edu

Keywords: Galápagos, Mantle Plume, Geochemistry, Isotopic Zonation, Mantle Dynamics

Highlights:

- There are temporal variations in the degree of isotopic enrichment associated with different 'stripes' in the Galápagos Mantle Plume.
- Shallow mantle processes control the average depth of melting and the degree of geochemical enrichment in the resulting basalts.
- Northward migration of the Galápagos Spreading center above the plume center has modified the temporal trends in lava chemistry in predictable ways.
- Therefore, there is no need to invoke temporal variations in plume chemistry and source proportions over the last ~15 Myrs in the Galápagos.

Abstract

Some hotspot tracks, such as those formed by the Hawai'i and Galápagos mantle plumes, exhibit long-lived cross-track isotopic zonation, thought to reflect the streaking out of heterogeneous material in the plume conduit during upwelling. In lavas associated with the Galápagos mantle plume, three geochemical domains, present for at least 15 Myr, have been identified: northern, southern and central. The most extreme isotopic enrichments are observed in the northern domain of the Cocos Ridge at ~15 Ma, and in the southern domain of the Galápagos Archipelago at the present day. Owing to the northward migration of the Galápagos Spreading Centre above the plume since ~20 Ma, this relationship suggests that geochemical enrichment in the Galápagos basalts is always greatest above the region of the plume furthest from the nearby mid-ocean ridge. Here we demonstrate that the temporal variations in geochemical enrichment associated

with Galápagos plume stripes likely reflect "shallow mantle control" associated with differences in the mean depth of melting. We conduct forward melting models of a mixed peridotite-pyroxenite mantle to calculate the isotopic composition of the resulting melts formed under two mantle flow regimes. Our results demonstrate that variations in the average pressure of melt generation, due to the influence of the nearby ridge axis, may explain the range of isotopic compositions across ~15 Ma of Galápagos plume-related volcanism. The patterns of isotopic zonation observed along the hotspot track strongly confirm the paradigm of persistent plume striping, with variations in the degree of geochemical enrichment modulated by shallow mantle processes.

Introduction

Mantle plumes and associated ocean-island basalts (OIBs) provide important insights into the composition, dynamics, and heterogeneity of the Earth's convecting mantle (Hofmann, 1997; Jackson et al., 2008; Weis et al., 2023; White et al., 1993; White and Hofmann, 1982). Variations in the isotopic compositions of OIBs suggest contributions from deep (primordial?) mantle reservoirs, recycled crust and re-fertilized lithospheric mantle, indicating a complex and heterogeneous structure derived from the lower mantle (Cabral et al., 2013; Homrighausen et al., 2020; Jackson et al., 2008; Williams et al., 2015; Zindler and Hart, 1986). These components are entrained into rising mantle plumes and, depending on their viscosity, are likely stretched into thin streaks of material that melt along with the plume matrix at shallow pressures, giving rise to a range of isotopic compositions measured at the surface (Farnetani et al., 2012, 2018; Harpp et al., 2014a; Hoernle et al., 2000; Kerr and Mériaux, 2004; Lohmann et al., 2009).

Spatial zonation in the composition of mantle plume-related basaltic lavas suggest the presence of distinct geochemical domains or plume 'stripes', characterized by the presence of spatially-variable chemical and lithological heterogeneities (Abouchami et al., 2005; Chauvel et al., 2012; Gleeson et al., 2021; Harpp et al., 2014a; Harpp and Weis, 2020; Hoernle et al., 2000, 2015; Huang et al., 2011; Payne et al., 2013; Weis et al., 2011). Classic examples are the Galápagos (Hoernle et al., 2000; Werner et al., 2003), where three compositionally enriched 'domains' have been observed, and Hawai'i, where basalts associated with the Loa trend display enriched isotopic compositions relative to the Kea trend (Abouchami et al., 2005; Harpp and Weis, 2020; Tatsumoto, 1978). The presence of compositional striping is now recognized as a common feature of many plume structures worldwide, including the Marquesas, Easter, Samoa, and Tristan-Gough Island/seamount chains, and may be connected to seismically identified heterogeneities in the Earth's lower mantle (Gleeson et al., 2021; Harpp et al., 2014b; Homrighausen et al., 2023, 2020; Rohde et al., 2013; Weis et al., 2023)

Laboratory tank experiments and numerical models of thermal or thermo-chemical plumes arising from the base of the mantle provide support for plume zonation/striping (Farnetani et al., 2012; Farnetani and Hofmann, 2009; Farnetani and Samuel, 2005; Kerr and Mériaux, 2004; Lohmann et al., 2009). For example, Farnetani and Hofmann (2009) show that geochemically distinct material from the lowermost mantle, once entrained into a plume conduit, gets stretched into long filaments. This process leads to long-lasting spatial zonation of the plume conduit, which affects the spatio-temporal isotopic variability of erupted lavas.

Within individual plume stripes the isotopic composition of basalts is not constant, but instead varies as a function of position above the plume conduit and orientation of plume motion relative to each chemical domain (Farnetani et al., 2012; Hanano et al., 2010). What is less certain, however, is whether adjustments in plume chemistry (that is, changes in the composition of plume heterogeneities or proportions of different components) are also required to explain temporal variations within an individual plume stripe. If variations in mantle plume composition through time can be identified, this could have significant implications for the size, persistence, and/or distribution of streaked heterogeneities within plume structures, and could also help identify the "end-member" stripe compositions.

In this study, we examine potential changes in the composition of plume stripes associated with the Galápagos mantle plume. Specifically, we compare the composition of basalts associated with the Galápagos Archipelago (formed during the last 3 Ma) to those erupted at ~15 Ma along the northern Galápagos plume track (Cocos Ridge; Fig. 1). We use numerical mantle melting models, namely the Python3 package pyMelt (Matthews et al., 2022), to investigate the origin of temporal variations in basalt chemistry. Our analysis focuses on the northern isotopic domain, identified by Hoernle et al. (2000) and Werner et al. (2003), and examines whether differences in the mean melting depth could cause the variations in geochemical enrichment associated with the northern domain basalts over the last ~15 Ma. Our results demonstrate that, despite substantial variations in the degree of isotopic enrichment, the ~15 Ma record of Galápagos plume-related volcanism can be straightforwardly explained by variations in the mean melting pressure, without having to invoke variations in plume composition and/or the proportion of different plume components.

This preprint has undergone one round of review in *Earth and Planetary Science Letters* and has been accepted for publication (as of April 2024)

Geological Background

Basalts erupted along the Galápagos hotspot track contain melt contributions from at least three isotopically-enriched mantle reservoirs, together with a depleted plume component (Geist et al., 1988; Gibson et al., 2012; Gleeson et al., 2021, 2020; Harpp and White, 2001; Hoernle et al., 2000; White et al., 1993). Importantly, the three isotopically-enriched regions are geographically separate and spatially-distinct (Hoernle et al., 2000; White et al., 1993). In the northern Galápagos, high $^{208}Pb/^{206}Pb$ ratios – found in basalts from the islands of Pinta, Wolf, Darwin, and surrounding seamounts – characterize the "northern domain" (Fig. 2). In the western Galápagos, Sr, Pb, and Nd isotope ratios, similar to the globally defined FOZO or 'C' plume component (Hanan and Graham, 1996), together with elevated $^{3}He/^{4}He$ ratios define the "central domain" (Kurz and Geist, 1999). Finally, in the southern Galápagos, radiogenic Pb isotope ratios (e.g., $^{206}Pb/^{204}Pb > 19.5$) associated with the island of Floreana and, to a lesser extent, the volcanoes of Sierra Negra and Cerro Azul on Isabela define the "southern domain" (Harpp et al., 2014a; Harpp and White, 2001; Hoernle et al., 2000).

Volcanism in the Galápagos Archipelago is the product of a near-ridge ("off-axis") mantle plume (see Fig. 1). The plume center is currently located about 150 – 250 km south of the Galápagos Spreading Center (GSC); a mid-ocean ridge spreading center separating the Cocos and Nazca tectonic plates (Canales et al., 2002; Gibson et al., 2015; Gleeson and Gibson, 2021; Harpp et al., 2003; Mittal and Richards, 2017; Mittelstaedt et al., 2014, 2012; Schilling et al., 2003, 1982). However, relative motion between the plume and ridge has led to substantial changes in the plume-ridge geometry through time.

Volcanism above the mantle plume and plume-ridge interaction have led to the formation of two separate plume tracks, the NE-SW orientated Cocos Ridge on the Cocos plate, and the E-W orientated Carnegie Ridge on the Nazca plate (Harpp et al., 2005; Hoernle et al., 2000; Werner et al., 2003). Between them, these aseismic ridges preserve a ~20 Myr record of plume volcanism and plume-ridge interaction, tracking the evolving tectonic setting of the Galápagos mantle plume and GSC during this period (Fig. 1). Furthermore, the relative volume of these ridges, and the age of plume-related basalts relative to the underlying oceanic crust formed at the ridge axis, provide important insights into the relative motion of the GSC and Galápagos mantle plume over the last ~20 Myrs (Werner et al. 2003).

The E-W (and originally NE-SW) orientation of the GSC combined with the eastward motion of the Nazca plate and north-east motion of the Cocos plate has resulted in a net northward migration of the GSC, relative to the Galápagos mantle plume, since ~20 Ma (Mittelstaedt et al., 2012; Werner et al. 2003). This northward progression, however, is complicated by a series of ridge jumps that reflect the capture of the GSC by the mantle plume during its northward migration. Existing plate reconstructions indicate that, at ~19.5 Ma, the GSC was likely anchored to the northern portion of the Galápagos plume (Werner et al. 2003), leading to heighted volcanism on the Nazca tectonic plate and increased volume of the Carnegie Ridge and associated Malpelo Ridge. Around ~14.5-15 Ma, the orientation and location of plate separation changed significantly, moving the center of plate separation to the southern margin of the mantle plume (Fig. 3; Werner et al. 2003). Until 11-12Ma volcanism continued with the plume positioned to the north of the spreading center, leading to a reduced volume of the Carnegie

Ridge and heightened activity along the Cocos Ridge (this is evidenced by the notable saddle in the Carnegie Ridge in bathymetric maps – see Orellana-Rovirosa and Richards (2018), for an analysis of how this process has modulated the complementary volumes of volcanism along the two ridges in time). The new plume-ridge orientation resulted in an increased volume to the northern Cocos Ridge – now located near the Costa Rica coastline – and the emergence of a paleo-archipelago in this region at around 13 – 14.5 Ma (Werner et al., 2003, 1999). Notably, basalts erupted as part of the northern Cocos Ridge are older than the underlying oceanic crust (15 – 19 Ma with increasing age to the north, derived from magnetic stripes; Barckhausen et al., 2001; Werner et al., 2003), supporting the interpretation that these basalts formed from plume-related volcanism north of the spreading axis.

After ~11 Ma, likely due to the passage of a ridge offset across the plume center (Werner et al. 2003), the axis of plate spreading migrated northward relative to the Galápagos mantle plume. Ultimately, this resulted in a situation not dissimilar to present-day Iceland, with the mantle plume located almost directly beneath the ridge axis. The northward motion of the GSC relative to the mantle plume caused enhanced melting south of the ridge axis and renewed growth of the Carnegie Ridge on the Nazca plate. Since ~ 5Ma, the GSC has migrated to the north of the Galápagos plume, with the distance between the plume and ridge controlled by a series of south-ward ridge jumps (Mittelstaedt et al. 2012). Ultimately, this has led to further broadening of the Carnegie Ridge and the construction of the present-day Galápagos Platform and volcanic islands (Fig. 2).

In this study, we focus our analyses and models onto two of the time periods outlined above, reflecting in large part the availability of geochemical data as per Hoernle et al (2000) and Werner et al. (2003). First, we focus on basalts along the Cocos Ridge that erupted at ~13 – 14.5 Ma. These samples, collected from the northernmost portion of the Cocos Ridge near Costa Rica-Panama coastline, are found on oceanic crust that is ~2 – 5 Ma older than the plume-related lavas and formed when the GSC was located near the southern margin of the upwelling plume stem. Second, we consider the isotopic composition of basalts found in the present-day Galápagos Archipelago, with the center of the upwelling plume stem >100 km south of the GSC. These two suites of plume-related lavas represent an interesting point of comparison and allow us to investigate how the position of the mantle plume relative to the GSC influences the enrichment of erupted plume-related material.

Importantly, spatially distinct northern, central, and southern isotopic domains – linked to those observed in the Galápagos Archipelago – have been identified in the northern Cocos Ridge lavas by Hoernle et al. (2000). As a result, it has been proposed that the spatial distribution of the three isotopically enriched components in the Galápagos mantle plume has been stable for at least ~15 Myrs. However, significant variations in the degree of isotopic enrichment of basalts within each domain do exist, which raises uncertainties regarding the stability and longevity of plume striping. Most notably, the basalts assigned to the northern plume domain along the Cocos Ridge have Sr, Nd, and Pb isotope signatures that are outside the range of values measured in any <3 Ma basalt from the Galápagos Archipelago (but retain the high $^{208}Pb/^{206}Pb$ characteristics of the northern domain; Hoernle et al., 2000). In fact, these isotopic compositions lie outside the range that could be achieved by mixing previously estimated end members in the Galápagos plume

(Harpp and White, 2001; Hoernle et al., 2000). In contrast, the Pb and Sr isotope compositions of basalts from the Galápagos island of Floreana (southern domain) are more radiogenic than those measured in basalts assigned to the southern domain on the Cocos Ridge (Harpp et al., 2014a; Hoernle et al., 2000). In this study, we provide a detailed analysis of variable geochemical enrichment associated with the different stripes of the Galápagos mantle plume, investigating whether the changes in chemical enrichment over 15 Ma require modifications in the plume source (e.g., changing plume chemistry and/or proportions), or instead result from physical variations in melting processes. In particular, we focus on the greater isotopic enrichment of northern domain lavas, relative to the southern domain, from the Cocos Ridge at ~15 Ma and *vice versa* for the present-day Galápagos-ridge system where the southern domain is more enriched relative to the northern domain.

Methods and Modeling

The primary objective of this study is to evaluate how variations in melting parameters (e.g., the average depth of melting) influence the isotopic composition of the resulting magmas. To do so, we use the Python package pyMelt, which uses empirical parameterizations of the melting behaviour for various mantle lithologies to simulate partial melting of a multi-component mantle (Matthews et al., 2022). pyMelt assumes that the different sources are in thermal equilibrium but are chemically isolated, this is a reasonable assumption since thermal diffusivity is much faster than chemical diffusivity. For each lithology, the trace element content of the melt is calculated by pyMelt via built-in partition coefficients taken from Gibson and Geist (2010), and assumptions about the mineral proportions in the different source lithologies.

All models presented in this study assume a simple 2-component mantle, with an isotopically depleted lherzolite (representing the plume "matrix") and an isotopically enriched pyroxenite (representing streaks of recycled crust and/or refertilized lithosphere; Hoernle et al., 2000; Sobolev et al., 2007; Sun et al., 2020). The melting behavior of these two source components is modeled in pyMelt using the melting parameterizations of the KLB-1 lherzolite and KG1 pyroxenite from Matthews et al. (2021) (Fig. 4). The potential temperature of the Galápagos mantle plume (T_p) was set at 1400-1420 ºC, with values between 1420 and 1500ºC also tested. The pressure of melt cessation, here representing the base of the lithosphere, was set between 1.3 – 1.9 GPa, consistent with geochemistry-constrained estimates of lithospheric thickness beneath the Galápagos Archipelago (Gibson and Geist, 2010).

Here we examine the extent to which variations in the melting process affect the chemistry of erupted basalts. First, we consider the chemistry of melts produced during transfer of material from the plume stem towards the ridge axis on the near-ridge margin of the upwelling plume stem (Fig. 5, blue arrows). In this scenario we assume that the upwelling velocity of plume material passing beneath the near-ridge region (i.e., in the northern Galápagos) is constant, controlled by the upwelling of material into the region created by the spreading plates (i.e., passive upwelling in near-ridge settings). This is supported by the geodynamic modelling of Ito and Bianco (2014), whose results demonstrate that across a ~100 km depth interval there is little to no change in the upwelling velocity of material during lateral transport to the ridge axis. Throughout the rest of the paper, this scenario is referred to as "Model 1" or the "Ridge Flow Model".

Our second scenario considers the flow of mantle material on the side of the plume conduit that is furthest from the nearby spreading center (i.e., beneath Volcan Cerro Azul and Isla Floreana at the present day; Fig. 5, orange arrows). Here, gravitationally driven flow and plate separation do not contribute to the upwelling of plume material. Instead, there is a strong depth dependence to the upwelling velocity within the plume margin as the velocity vectors change from nearly vertical at the base of the melting region to approximately horizontal at the base of the mechanical lithosphere (Fig. 5). This scenario is described in detail by Ito and Mahoney (2005), and we utilize their model of depth dependent lateral flow rates to estimate variations in the relative melt production rate with pressure. Throughout the rest of the paper, we refer to this scenario as "Model 2" or the "Plume Flow Model". Models 1 and 2 are shown graphically in Fig. 5, which was adapted from a 3D geodynamic model of plume-ridge interaction by Ito and Bianco (2014).

To calculate the isotopic and trace element composition of the accumulated melts we first need to make some assumptions regarding the trace element and isotopic compositions of the different source regions. The isotopic composition of the depleted lherzolite component in the Galápagos mantle plume is taken from Harpp and White (2001), with the trace element chemistry set to that of the Workman and Hart (2005) depleted MORB mantle (DMM). The rare earth element (REE) composition of the enriched, pyroxenitic component in the northern Galápagos plume domain was set as a 50:50 mixture of the Stracke et al. (2003) estimate for subducted basaltic crust and the DMM. The Sr and Pb contents of this component were treated independently, with the "enrichment factor" of each element (i.e., $[Sr]^{pyroxenite}/[Sr]^{lherzolite}$) iteratively adjusted to improve

the fit between the models and observations. Finally, because we focus on the northern Galápagos domain, the isotopic signature of the pyroxenite component was set to the composition of the most enriched value measured in basalts from the northern domain of the Cocos Ridge (Hoernle et al., 2000; Werner et al., 2003).

To examine the spread of compositions that may be produced by mantle melting in the two models shown in Figure 5, we used two approaches to simulate the variability in erupted basalt chemistry. First, we use a Monte Carlo approach to sample uniform prior distributions for the plume potential temperature (1400-1420^{o}C), the pressure of melt cessation (1.3–1.5 GPa, Model 1; 1.4-1.9 GPa, Model 2), and the source proportions (pyroxenite fraction, X_{px}=0.12 – 0.13; bounds iteratively adjusted to best fit the natural data). We also run a separate series of models to examine how slight variations in these core variables influence the composition of the mean accumulated melt phase, with the source proportion of pyroxenite having the dominant control on the predicted isotopic composition of melts produced by each Model (Fig. 6). Second, we simulate incomplete homogenization of mantle melts following the approach of Rudge et al. (2013), using a Dirichlet mixing function to examine random mixing of mantle melts (with the probability of sampling each melt determined by proportion of melt produced at each depth; Fig. 5). The extent of homogenization in these calculations is described by a single parameter N, where N = 1 indicates complete isolation (no mixing) of all melts produced in the melting region, whereas N = ∞ represents complete homogenization of all mantle melts (see Supplementary Material).

Results

Variations in isotopic enrichment between basalts from the Galápagos Archipelago and the ~13 – 15 Ma segment of the Cocos Ridge can be summarized by two main differences: (i) greater isotopic enrichment of the northern domain along the Cocos Ridge, and (ii) greater enrichment of the southern domain in the modern-day Galápagos Archipelago (Harpp et al., 2014, 2005; Hoernle et al., 2000; Werner et al., 2003). The temporal changes in isotopic compositions of erupted basalts could, in theory, have several possible origins, the simplest of which would be variations in the composition of the mantle source (either through changing proportions of mantle sources or variations in the composition of mantle end members; Fig. 6b). This explanation appears to be supported by the extreme isotopic compositions observed in the northern domain of the Cocos Ridge (Hoernle et al., 2000), where Sr-Pb-Nd isotope values plot outside the field of compositions enclosed by previously proposed mantle end-member compositions associated with the Galápagos plume (Harpp and Weis, 2020; Harpp and White, 2001). However, the 15 Ma northern domain Cocos Ridge lavas are characterized by the same high $^{208}Pb/^{206}Pb$ signature that is typical of <3 Ma basalts from the islands of Wolf, Darwin, Pinta, surrounding seamounts, and western GSC (Figs. 2 & 3). It is difficult to explain how this signature is maintained if the composition of the northern domain mantle source components vary through time, barring appeal to coincidence. Instead, this implies a stable "enriched" mantle component in the northern Galápagos across this 15Ma record of Galápagos plume volcanism, with a source isotopic signature that is more enriched than that proposed for the "Wolf-Darwin" component of Harpp and White (2001). Compositional variations in basaltic lavas must, therefore, originate through temporal fluctuations in mantle source proportions, or "shallow mantle" processes such as the mean pressure of melting. Here we consider the second option, tracking melt compositions formed during flow towards a nearby spreading center ("Model 1")

and beneath a thicker lithospheric 'lid' on the far side of the plume stem ("Model 2"). For these calculations we focus solely on the northern isotopic plume domain, due to ongoing uncertainties in the lithology and origin of the southern plume component (Gleeson et al., 2021; Vidito et al., 2013), but emphasize that our results are applicable to any scenario where an isotopically enriched, more fertile mantle component starts to melt at greater pressures than a depleted peridotite matrix during adiabatic decompression.

For each model we ran 200 simulations, randomly varying the mantle potential temperature, lithospheric thickness, and source pyroxenite component as described above. In every simulation we 'sampled' the magmas formed in the melting region 200 times using a Dirichlet Mixing Model, following the method outlined in Rudge et al. (2013), to estimate the composition and compositional variation of erupted magmas (N=2000). Ultimately this approach generated 40,000 hypothetical compositions for magmas formed in each model. The results shown in Figure 7 demonstrate a significant shift in the average pressure of melting from ~2.3 GPa in Model 1 to 3.15 GPa in Model 2, driven by differences in the modelled rates of melt formation at each depth with variations in lithospheric thickness having a secondary influence (Fig. 6, 7). The compositions generated in Model 2 consistently display more radiogenic Sr and Pb isotope signatures and less radiogenic Nd isotope signatures compared to Model 1 (Fig. 7).

Isotope plots demonstrate that the Model 1 melts have isotopic compositions that closely resemble basalts from the island of Pinta and surrounding submarine ridge (Fig. 7). The results from Model 2 simulations stretch to more isotopically enriched compositions, overlapping with the range of values measured in northern domain basalts from the Cocos Ridge. Notably, the

compositions predicted by Model 2 simulations are outside the range of radiogenic isotope values measured anywhere in the Galápagos Archipelago. As a result, our simulations conclusively show that the isotopic composition of basalts from the northern Galápagos island of Pinta and the northern domain of the Cocos Ridge can be recreated by the two melting models considered in this study. Furthermore, owing to the greater contribution of high-pressure melts in Model 2 – where lower degrees of melting in the presence of garnet occurs – significant trace element enrichment, relative to Model 1, is observed in our simulations. Because of the large uncertainty in the trace element content of the different mantle sources we don't try to directly recreate the trace element profiles of the Galápagos and Cocos Ridge lavas, but instead consider the trends in trace element enrichment/depletion between the two models. Model 2 melts display a ~1.3 times enrichment in the $[Dy/Yb]_n$ ratio (where n indicates normalization to the primitive mantle of Sun and McDonough, 1989), consistent with the enrichment observed in the Cocos Ridge northern domain lavas relative to Pinta. These middle-to-heavy REE ratios are predominantly controlled by the presence of garnet in the mantle source and, therefore, track variations in the mean depth of melting consistent with the hypothesis presented here. Our models also demonstrate significant enrichment in the light REE in the Model 2 melts (~1.4 – 1.5X). This enrichment is slightly less than the 2X enrichment observed between the Cocos Ridge northern domain and Pinta lavas, which might originate through the absence of hydrous melting regimes in our models and or slight errors in the source trace element contents. Nevertheless, the differences between Model 1 and Model 2 melts recreate both the isotopic and broad-scale trace element differences between the Cocos Ridge northern domain and Pinta lavas.

In summary, our results demonstrate that the composition of basalts from both the island of Pinta (northern Galápagos Archipelago) and the northern plume domain of the Cocos Ridge can be reproduced without having to invoke variations in mantle source chemistry, proportions, or potential temperature (Fig. 6). Instead, we find that variations in the mean melting depth – driven by predictable variations in mantle flow rates on either side of the Galápagos plume stem – control the geochemical enrichment of individual plume stripes. Furthermore, the spread of data at each location can be reproduced by accounting for minor stochastic variations in source proportions, melting depths and mantle potential temperatures, as well as incomplete mixing and homogenization of the melts produced (Fig. 7). To best fit the Galápagos Archipelago and Cocos Ridge data, we propose that the northern domain in the Galápagos plume contains ~12.5 % pyroxenite streaks in a depleted peridotite matrix. We also find that the northern enriched pyroxenite source is likely represented by the isotopic composition of the most enriched northern domain basalt from the Cocos Ridge. We stress that these values are non-unique solutions, as different assumptions regarding the source lithology/volatile content etc. will likely influence the estimated source composition. The actual end member composition of course could be more extreme, lying on the northern domain array at more radiogenic Sr and Pb and less radiogenic Nd isotopic composition. Nevertheless, we emphasize that the geochemical variations within the Galápagos plume stripes can successfully be modelled without temporal changes in plume chemistry/proportions.

Discussion

The presence of spatial zonation of isotopic domains in mantle plumes has been documented at several locations worldwide, with variations in the composition of basalts erupted in each zone

linked to the distribution of heterogeneities within the plume structure and/or the influence of plume dynamics on melt production and/or extraction (e.g., Chauvel et al., 2012; Farnetani et al., 2012; Gleeson et al., 2021; Lohmann et al., 2009; Weis et al., 2011). Here we have shown that, despite large and conspicuous variations in basalt chemistry, the end member compositions of plume stripes within the Galápagos Archipelago are stable over timescales of at least ~15 Myrs. We find that variations in the isotopic ratio of basalts originating from the northern component of the Galápagos plume result from temporal changes in mean depth of melting, related to the south-to-north motion of the GSC across the plume. Our results confirm the presence of persistent plume striping in the Galápagos Archipelago and provide new constraints on the end-member isotopic compositions of enriched plume components. Furthermore, our results indicate that the northern domain is broadly homogeneous on timescales up to ~15 Myrs.

Our results do not include a full dynamical simulation of plume-ridge interaction in the Galápagos region, so that melting in the Galápagos mantle plume could, in reality, deviate from either "Model" proposed here. Nevertheless, our models demonstrate the importance of considering melting parameters and mantle dynamics when inverting OIB geochemistry for mantle geochemical signatures.

The presence of compositional striping in mantle plumes has been identified at many locations worldwide (e.g., Abouchami et al., 2005; Chauvel et al., 2012; Harpp and Weis, 2020; Hoernle et al., 2000; 2015; Huang et al., 2011; Rohde et al., 2013; Weis et al., 2011), with many plume systems showing temporal trends in the degree of geochemical enrichment associated with individual plume stripes (Chauvel et al., 2012; Homrighausen et al., 2019). Here we have shown

that variable enrichment within plume stripes of the Galápagos Archipelago can be explained by shallow mantle processes modulating the mean depth of melting and, therefore, the degree of chemical enrichment. Following on from this analysis we suggest that compositional variations of lavas associated with stripes at other plume systems worldwide should be critically examined in a similar manner. This could reveal where, and when, chemical variations are explained through modulation of melt chemistry by shallow mantle processes and where temporal variations in plume chemistry and/or source proportions are required. As a result, further analysis of temporal variations in plume stripe chemical enrichment could help to quantify the typical length scales of streaked heterogeneities, originating in the Earth's deep mantle, in upwelling mantle plumes.

We suggest that this work should start with other near-ridge plume systems, such as the Walvis-Ridge – Tristan-Gough plume track, where compositional stripes have been observed (Homrighausen et al., 2019). Expansion of this analysis to intra-plate plume systems, however, is also encouraged. For example, the Marquesas Islands in French Polynesia are split into two geochemical tracks named the "Fatu Hiva" and "Ua Huka" groups (Huang et al., 2011; Chauvel et al., 2012). Within each track there is distinct variability in erupted compositions and clear temporal patterns over ~5 Myr in the overall isotopic enrichment of erupted basalts. Temporal variations in lithospheric thickness and/or plume dynamics – such as in the Galápagos – are unlikely to explain these trends owing to the greater lithospheric age and distance from any plate boundary. Instead, subtle variations in other melting parameters, including mantle potential temperatures, might explain these isotopic changes without having to invoke differences in the composition and/or source proportions of the mantle plume. While we show variations in plume

T_p have a moderate influence on the isotopic composition of basalts erupted in the Galápagos (Fig. 6), we suggest that variations in plume temperatures (and other melting parameters) might have a far greater influence in systems where the melt fraction of isotopically depleted plume components is low (typically <2%). For example, the Marquesas Islands are characterized by a relatively low erupted flux (1 – 2 orders of magnitude lower than Hawai'i) and alkali-rich basalts, indicating that small variations in melting processes could have a strong influence on the isotopic composition of erupted basalts in this region (Chauvel et al., 2012).

Conclusions

Observed variations in the intensity of isotopic zonation of Galápagos basalts over the last 15 Ma can be accounted for by variations in mean depth of melting during the northward migration of the GSC above the Galápagos plume stem. The fact that these observations can be explained so straightforwardly provides powerful verification of the elegant theoretical concept of mantle plume geochemical striping (zonation), demonstrates the time-persistence of these stripes over at least the past 15 Ma, allows us to constrain the end-member geochemical signatures of these stripes, and therefore suggests that similar variations can be mapped and modeled along other hotspot tracks, perhaps especially those that are near mid-ocean ridges, where temporal variations in lithospheric thickness may have the most effect. This should ultimately lead to a more refined definition of the nature of the true "end member" geochemical source regions for mantle plumes, and their interaction with ambient mantle as they ascend from the core-mantle boundary and undergo partial melting beneath the lithosphere.

Acknowledgements

M.G. and M.R. wish to acknowledge support from the Esper Larsen Jr. Research Fund at UC Berkeley, and discussions with Alex Bearden on plume striping worldwide. We thank Kevin Konrad and Jo Whittaker for their constructive reviews, which greatly helped to improve the manuscript, as well as Feng-Zhen Teng for editorial handling.

Data and Code availability

All code used for the production of models and figures used in this study is currently available on GitHub (https://github.com/gleesonm1/GleesonEtAl_PlumeStriping), and is archived on Zenodo https://doi.org/10.5281/zenodo.18355128. Data used in this study is taken from (Allan and Simkin, 2000; Bow and Geist, 1992; Geist et al., 2006, 2002; Gibson et al., 2012; Gibson and Geist, 2010; Harpp et al., 2003; Harpp and Weis, 2020; Harpp and White, 2001; Hoernle et al., 2000; Kurz and Geist, 1999; McBirney and Williams, 1969; Saal et al., 2007; Standish et al., 1998; Teasdale et al., 2005; White et al., 1993)

CRediT authorship contribution statement

Matthew Gleeson: Conceptualization, Writing – original draft, Formal analysis, Methodology; **Mark Richards:** Conceptualization, Writing – review & editing; **Cinzia Farnetani:** Writing – review & editing; **Kaj Hoernle:** Writing – review & editing**; Sally Gibson:** Writing – review & editing.

References

Abouchami, W., Hofmann, A.W., Galer, S.J.G., Frey, F.A., Eisele, J., Feigenson, M., 2005. Lead isotopes reveal bilateral asymmetry and vertical continuity in the Hawaiian mantle plume. Nature 434, 851–856. https://doi.org/10.1038/nature03402

Allan, J.F., Simkin, T., 2000. Fernandina Volcano's evolved, well-mixed basalts: Mineralogical and petrological constraints on the nature of the Galapagos plume. J. Geophys. Res. Solid Earth 105, 6017–6041. https://doi.org/10.1029/1999JB900417

Barckhausen, U., Ranero, C.R., von Huene, R., Cande, S.C., Roeser, H.A., 2001. Revised tectonic boundaries in the Cocos Plate off Costa Rica: Implications for the segmentation of the convergent margin and for plate tectonic models. J. Geophys. Res. Solid Earth 106, 19207–19220. https://doi.org/10.1029/2001JB000238

Bow, C.S., Geist, D.J., 1992. Geology and petrology of Floreana Island, Galapagos Archipelago, Ecuador. J. Volcanol. Geotherm. Res., Special Issue in Honour of Alexander R. McBirney 52, 83–105. https://doi.org/10.1016/0377-0273(92)90134-Y

Cabral, R.A., Jackson, M.G., Rose-Koga, E.F., Koga, K.T., Whitehouse, M.J., Antonelli, M.A., Farquhar, J., Day, J.M.D., Hauri, E.H., 2013. Anomalous sulphur isotopes in plume lavas reveal deep mantle storage of Archaean crust. Nature 496, 490–493. https://doi.org/10.1038/nature12020

Canales, J.P., Ito, G., Detrick, R.S., Sinton, J., 2002. Crustal thickness along the western Galápagos Spreading Center and the compensation of the Galápagos hotspot swell. Earth Planet. Sci. Lett. 203, 311–327. https://doi.org/10.1016/S0012-821X(02)00843-9

Chauvel, C., Maury, R.C., Blais, S., Lewin, E., Guillou, H., Guille, G., Rossi, P., Gutscher, M., 2012. The size of plume heterogeneities constrained by Marquesas isotopic stripes.

493 Geochem. Geophys. Geosystems 13, 2012GC004123.
494 https://doi.org/10.1029/2012GC004123
495 Farnetani, C.G., Hofmann, A.W., 2009. Dynamics and internal structure of a lower mantle
496 plume conduit. Earth Planet. Sci. Lett. 282, 314–322.
497 https://doi.org/10.1016/j.epsl.2009.03.035
498 Farnetani, C.G., Hofmann, A.W., Class, C., 2012. How double volcanic chains sample
499 geochemical anomalies from the lowermost mantle. Earth Planet. Sci. Lett. 359–
500 360, 240–247. https://doi.org/10.1016/j.epsl.2012.09.057
501 Farnetani, C.G., Hofmann, A.W., Duvernay, T., Limare, A., 2018. Dynamics of rheological
502 heterogeneities in mantle plumes. Earth Planet. Sci. Lett. 499, 74–82.
503 https://doi.org/10.1016/j.epsl.2018.07.022
504 Farnetani, C.G., Samuel, H., 2005. Beyond the thermal plume paradigm. Geophys. Res.
505 Lett. 32. https://doi.org/10.1029/2005GL022360
506 Geist, D., Chadwick, W., Johnson, D., 2006. Results from new GPS and gravity monitoring
507 networks at Fernandina and Sierra Negra Volcanoes, Galápagos, 2000–2002. J.
508 Volcanol. Geotherm. Res., The Changing Shapes of Active Volcanoes 150, 79–97.
509 https://doi.org/10.1016/j.jvolgeores.2005.07.003
510 Geist, D., White, W.M., Albarede, F., Harpp, K., Reynolds, R., Blichert-Toft, J., Kurz, M.D.,
511 2002. Volcanic evolution in the Galápagos: The dissected shield of Volcan Ecuador.
512 Geochem. Geophys. Geosystems 3, 1 of 32–32 32.
513 https://doi.org/10.1029/2002GC000355
514 Geist, D.J., White, W.M., McBirney, A.R., 1988. Plume-asthenosphere mixing beneath the
515 Galapagos archipelago. Nature 333, 657–660. https://doi.org/10.1038/333657a0
516 Gibson, S.A., Geist, D., 2010. Geochemical and geophysical estimates of lithospheric
517 thickness variation beneath Galápagos. Earth Planet. Sci. Lett. 300, 275–286.
518 https://doi.org/10.1016/j.epsl.2010.10.002
519 Gibson, S.A., Geist, D.G., Day, J.A., Dale, C.W., 2012. Short wavelength heterogeneity in the
520 Galápagos plume: Evidence from compositionally diverse basalts on Isla Santiago.
521 Geochem. Geophys. Geosystems 13. https://doi.org/10.1029/2012GC004244
522 Gibson, S.A., Geist, D.J., Richards, M.A., 2015. Mantle plume capture, anchoring, and
523 outflow during Galápagos plume-ridge interaction. Geochem. Geophys.
524 Geosystems 16, 1634–1655. https://doi.org/10.1002/2015GC005723
525 Gleeson, M., Soderman, C., Matthews, S., Cottaar, S., Gibson, S., 2021. Geochemical
526 Constraints on the Structure of the Earth's Deep Mantle and the Origin of the
527 LLSVPs. Geochem. Geophys. Geosystems 22, e2021GC009932.
528 https://doi.org/10.1029/2021GC009932
529 Gleeson, M.L.M., Gibson, S.A., 2021. Insights Into the Nature of Plume-Ridge Interaction
530 and Outflux of H2O From the Galápagos Spreading Center. Geochem. Geophys.
531 Geosystems 22, e2020GC009560. https://doi.org/10.1029/2020GC009560
532 Gleeson, M.L.M., Gibson, S.A., Williams, H.M., 2020. Novel insights from Fe-isotopes into
533 the lithological heterogeneity of Ocean Island Basalts and plume-influenced
534 MORBs. Earth Planet. Sci. Lett. 535, 116114.
535 https://doi.org/10.1016/j.epsl.2020.116114

536 Hanan, B.B., Graham, D.W., 1996. Lead and Helium Isotope Evidence from Oceanic
537 Basalts for a Common Deep Source of Mantle Plumes. Science 272, 991–995.
538 https://doi.org/10.1126/science.272.5264.991
539 Hanano, D., Weis, D., Scoates, J.S., Aciego, S., DePaolo, D.J., 2010. Horizontal and vertical
540 zoning of heterogeneities in the Hawaiian mantle plume from the geochemistry of
541 consecutive postshield volcano pairs: Kohala-Mahukona and Mauna Kea–Hualalai.
542 Geochem. Geophys. Geosystems 11. https://doi.org/10.1029/2009GC002782
543 Harpp, K.S., Fornari, D.J., Geist, D.J., Kurz, M.D., 2003. Genovesa Submarine Ridge: A
544 manifestation of plume-ridge interaction in the northern Galápagos Islands.
545 Geochem. Geophys. Geosystems 4. https://doi.org/10.1029/2003GC000531
546 Harpp, K.S., Geist, D.J., Koleszar, A.M., Christensen, B., Lyons, J., Sabga, M., Rollins, N.,
547 2014a. The Geology and Geochemistry of Isla Floreana, Galápagos, in: The
548 Galápagos. American Geophysical Union (AGU), pp. 71–117.
549 https://doi.org/10.1002/9781118852538.ch6
550 Harpp, K.S., Hall, P.S., Jackson, M.G., 2014b. Galápagos and Easter, in: The Galápagos.
551 American Geophysical Union (AGU), pp. 27–40.
552 https://doi.org/10.1002/9781118852538.ch3
553 Harpp, K.S., Wanless, V.D., Otto, R.H., Hoernle, K., Werner, R., 2005. The Cocos and
554 Carnegie Aseismic Ridges: a Trace Element Record of Long-term Plume–Spreading
555 Center Interaction. J. Petrol. 46, 109–133. https://doi.org/10.1093/petrology/egh064
556 Harpp, K.S., Weis, D., 2020. Insights Into the Origins and Compositions of Mantle Plumes: A
557 Comparison of Galápagos and Hawai'i. Geochem. Geophys. Geosystems 21,
558 e2019GC008887. https://doi.org/10.1029/2019GC008887
559 Harpp, K.S., White, W.M., 2001. Tracing a mantle plume: Isotopic and trace element
560 variations of Galápagos seamounts. Geochem. Geophys. Geosystems 2,
561 2000GC000137. https://doi.org/10.1029/2000GC000137
562 Hoernle, K., Rohde, J., Hauff, F., Garbe-Schönberg, D., Homrighausen, S., Werner, R.,
563 Morgan, J.P., 2015. How and when plume zonation appeared during the 132 Myr
564 evolution of the Tristan Hotspot. Nat. Commun. 6, 7799.
565 https://doi.org/10.1038/ncomms8799
566 Hoernle, K., Werner, R., Morgan, J.P., Garbe-Schönberg, D., Bryce, J., Mrazek, J., 2000.
567 Existence of complex spatial zonation in the Galápagos plume. Geology 28, 435–
568 438. https://doi.org/10.1130/0091-7613(2000)28%253C435:EOCSZI%253E2.0.CO;2
569 Hofmann, A.W., 1997. Mantle geochemistry: the message from oceanic volcanism. Nature
570 385, 219–229. https://doi.org/10.1038/385219a0
571 Homrighausen, S., Hoernle, K., Hauff, F., Hoyer, P.A., Haase, K.M., Geissler, W.H.,
572 Geldmacher, J., 2023. Evidence for compositionally distinct upper mantle plumelets
573 since the early history of the Tristan-Gough hotspot. Nat. Commun. 14, 3908.
574 https://doi.org/10.1038/s41467-023-39585-0
575 Homrighausen, S., Hoernle, K., Hauff, F., Wartho, J.-A., Van Den Bogaard, P., Garbe-
576 Schönberg, D., 2019. New age and geochemical data from the Walvis Ridge: The
577 temporal and spatial diversity of South Atlantic intraplate volcanism and its possible
578 origin. Geochim. Cosmochim. Acta 245, 16–34.
579 https://doi.org/10.1016/j.gca.2018.09.002

Homrighausen, S., Hoernle, K., Zhou, H., Geldmacher, J., Wartho, J.-A., Hauff, F., Werner, R., Jung, S., Morgan, J.P., 2020. Paired EMI-HIMU hotspots in the South Atlantic—Starting plume heads trigger compositionally distinct secondary plumes? Sci. Adv. 6, eaba0282. https://doi.org/10.1126/sciadv.aba0282

Huang, S., Hall, P.S., Jackson, M.G., 2011. Geochemical zoning of volcanic chains associated with Pacific hotspots. Nat. Geosci. 4, 874–878. https://doi.org/10.1038/ngeo1263

Ito, G., Bianco, T., 2014. Patterns in Galápagos Magmatism Arising from the Upper Mantle Dynamics of Plume-Ridge Interaction, in: The Galápagos. American Geophysical Union (AGU), pp. 245–261. https://doi.org/10.1002/9781118852538.ch13

Ito, G., Mahoney, J.J., 2005. Flow and melting of a heterogeneous mantle: 1. Method and importance to the geochemistry of ocean island and mid-ocean ridge basalts. Earth Planet. Sci. Lett. 230, 29–46. https://doi.org/10.1016/j.epsl.2004.10.035

Jackson, M.G., Hart, S.R., Saal, A.E., Shimizu, N., Kurz, M.D., Blusztajn, J.S., Skovgaard, A.C., 2008. Globally elevated titanium, tantalum, and niobium (TITAN) in ocean island basalts with high 3He/4He. Geochem. Geophys. Geosystems 9. https://doi.org/10.1029/2007GC001876

Kerr, R.C., Mériaux, C., 2004. Structure and dynamics of sheared mantle plumes. Geochem. Geophys. Geosystems 5. https://doi.org/10.1029/2004GC000749

Kurz, M.D., Geist, D., 1999. Dynamics of the Galapagos hotspot from helium isotope geochemistry. Geochim. Cosmochim. Acta 63, 4139–4156. https://doi.org/10.1016/S0016-7037(99)00314-2

Lohmann, F.C., Hort, M., Phipps Morgan, J., 2009. Flood basalts and ocean island basalts: A deep source or shallow entrainment? Earth Planet. Sci. Lett. 284, 553–563. https://doi.org/10.1016/j.epsl.2009.05.025

Matthews, S., Wong, K., Gleeson, M., 2022. pyMelt: An extensible Python engine for mantle melting calculations. Volcanica 5, 469–475. https://doi.org/10.30909/vol.05.02.469475

Matthews, S., Wong, K., Shorttle, O., Edmonds, M., Maclennan, J., 2021. Do Olivine Crystallization Temperatures Faithfully Record Mantle Temperature Variability? Geochem. Geophys. Geosystems 22, e2020GC009157. https://doi.org/10.1029/2020GC009157

McBirney, A.R., Williams, H., 1969. Geology and Petrology of the Galápagos Islands. Geological Society of America.

Mittal, T., Richards, M.A., 2017. Plume-ridge interaction via melt channelization at Galápagos and other near-ridge hotspot provinces. Geochem. Geophys. Geosystems 18, 1711–1738. https://doi.org/10.1002/2016GC006454

Mittelstaedt, E., Soule, A.S., Harpp, K.S., Fornari, D., 2014. Variations in Crustal Thickness, Plate Rigidity, and Volcanic Processes Throughout the Northern Galápagos Volcanic Province, in: The Galápagos. American Geophysical Union (AGU), pp. 263–284. https://doi.org/10.1002/9781118852538.ch14

Mittelstaedt, E., Soule, S., Harpp, K., Fornari, D., McKee, C., Tivey, M., Geist, D., Kurz, M.D., Sinton, C., Mello, C., 2012. Multiple expressions of plume-ridge interaction in the

623 Galápagos: Volcanic lineaments and ridge jumps. Geochem. Geophys. Geosystems
624 13. https://doi.org/10.1029/2012GC004093
625 Orellana-Rovirosa, F., Richards, M., 2018. Emergence/Subsidence Histories Along the
626 Carnegie and Cocos Ridges and Their Bearing Upon Biological Speciation in the
627 Galápagos. Geochem. Geophys. Geosystems 19, 4099–4129.
628 https://doi.org/10.1029/2018GC007608
629 Payne, J.A., Jackson, M.G., Hall, P.S., 2013. Parallel volcano trends and geochemical
630 asymmetry of the Society Islands hotspot track. Geology 41, 19–22.
631 https://doi.org/10.1130/G33273.1
632 Rohde, J., Hoernle, K., Hauff, F., Werner, R., O'Connor, J., Class, C., Garbe-Schönberg, D.,
633 Jokat, W., 2013. 70 Ma chemical zonation of the Tristan-Gough hotspot track.
634 Geology 41, 335–338. https://doi.org/10.1130/G33790.1
635 Rudge, J.F., Maclennan, J., Stracke, A., 2013. The geochemical consequences of mixing
636 melts from a heterogeneous mantle. Geochim. Cosmochim. Acta 114, 112–143.
637 https://doi.org/10.1016/j.gca.2013.03.042
638 Saal, A.E., Kurz, M.D., Hart, S.R., Blusztajn, J.S., Blichert-Toft, J., Liang, Y., Geist, D.J., 2007.
639 The role of lithospheric gabbros on the composition of Galapagos lavas. Earth
640 Planet. Sci. Lett. 257, 391–406. https://doi.org/10.1016/j.epsl.2007.02.040
641 Schilling, J.-G., Fontignie, D., Blichert-Toft, J., Kingsley, R., Tomza, U., 2003. Pb-Hf-Nd-Sr
642 isotope variations along the Galápagos Spreading Center (101°–83°W): Constraints
643 on the dispersal of the Galápagos mantle plume. Geochem. Geophys. Geosystems
644 4. https://doi.org/10.1029/2002GC000495
645 Schilling, J.-G., Kingsley, R.H., Devine, J.D., 1982. Galapagos Hot Spot-Spreading Center
646 System: 1. Spatial petrological and geochemical variations (83°W–101°W). J.
647 Geophys. Res. Solid Earth 87, 5593–5610. https://doi.org/10.1029/JB087iB07p05593
648 Sobolev, A.V., Hofmann, A.W., Kuzmin, D.V., Yaxley, G.M., Arndt, N.T., Chung, S.-L.,
649 Danyushevsky, L.V., Elliott, T., Frey, F.A., Garcia, M.O., Gurenko, A.A., Kamenetsky,
650 V.S., Kerr, A.C., Krivolutskaya, N.A., Matvienkov, V.V., Nikogosian, I.K., Rocholl, A.,
651 Sigurdsson, I.A., Sushchevskaya, N.M., Teklay, M., 2007. The Amount of Recycled
652 Crust in Sources of Mantle-Derived Melts. Science 316, 412–417.
653 https://doi.org/10.1126/science.1138113
654 Standish, J., Geist, D., Harpp, K., Kurz, M.D., 1998. The emergence of a Galápagos shield
655 volcano, Roca Redonda. Contrib. Mineral. Petrol. 133, 136–148.
656 https://doi.org/10.1007/s004100050443
657 Stracke, A., Bizimis, M., Salters, V.J.M., 2003. Recycling oceanic crust: Quantitative
658 constraints. Geochem. Geophys. Geosystems 4.
659 https://doi.org/10.1029/2001GC000223
660 Sun, P., Niu, Y., Guo, P., Duan, M., Chen, S., Gong, H., Wang, X., Xiao, Y., 2020. Large iron
661 isotope variation in the eastern Pacific mantle as a consequence of ancient low-
662 degree melt metasomatism. Geochim. Cosmochim. Acta 286, 269–288.
663 https://doi.org/10.1016/j.gca.2020.07.029
664 Sun, S. -s., McDonough, W.F., 1989. Chemical and isotopic systematics of oceanic basalts:
665 implications for mantle composition and processes. Geol. Soc. Lond. Spec. Publ.
666 42, 313–345. https://doi.org/10.1144/GSL.SP.1989.042.01.19

667 Tatsumoto, M., 1978. Isotopic composition of lead in oceanic basalt and its implication to
668 mantle evolution. Earth Planet. Sci. Lett., Trace Elements in Igneous Petrology 38,
669 63–87. https://doi.org/10.1016/0012-821X(78)90126-7
670 Teasdale, R., Geist, D., Kurz, M., Harpp, K., 2005. 1998 Eruption at Volcán Cerro Azul,
671 Galápagos Islands: I. Syn-Eruptive Petrogenesis. Bull. Volcanol. 67, 170–185.
672 https://doi.org/10.1007/s00445-004-0371-9
673 Vidito, C., Herzberg, C., Gazel, E., Geist, D., Harpp, K., 2013. Lithological structure of the
674 Galápagos Plume. Geochem. Geophys. Geosystems 14, 4214–4240.
675 https://doi.org/10.1002/ggge.20270
676 Weis, D., Garcia, M.O., Rhodes, J.M., Jellinek, M., Scoates, J.S., 2011. Role of the deep
677 mantle in generating the compositional asymmetry of the Hawaiian mantle plume.
678 Nat. Geosci. 4, 831–838. https://doi.org/10.1038/ngeo1328
679 Weis, D., Harpp, K.S., Harrison, L.N., Boyet, M., Chauvel, C., Farnetani, C.G., Finlayson,
680 V.A., Lee, K.K.M., Parai, R., Shahar, A., Williamson, N.M.B., 2023. Earth's mantle
681 composition revealed by mantle plumes. Nat. Rev. Earth Environ. 4, 604–625.
682 https://doi.org/10.1038/s43017-023-00467-0
683 Werner, R., Hoernle, K., Barckhausen, U., Hauff, F., 2003. Geodynamic evolution of the
684 Galápagos hot spot system (Central East Pacific) over the past 20 m.y.: Constraints
685 from morphology, geochemistry, and magnetic anomalies. Geochem. Geophys.
686 Geosystems 4, 2003GC000576. https://doi.org/10.1029/2003GC000576
687 Werner, R., Hoernle, K., van den Bogaard, P., Ranero, C., von Huene, R., Korich, D., 1999.
688 Drowned 14-m.y.-old Galápagos archipelago off the coast of Costa Rica:
689 Implications for tectonic and evolutionary models. Geology 27, 499–502.
690 https://doi.org/10.1130/0091-7613(1999)027%253C0499:DMYOGP%253E2.3.CO;2
691 White, W.M., Hofmann, A.W., 1982. Sr and Nd isotope geochemistry of oceanic basalts and
692 mantle evolution. Nature 296, 821–825. https://doi.org/10.1038/296821a0
693 White, W.M., McBirney, A.R., Duncan, R.A., 1993. Petrology and geochemistry of the
694 Galápagos Islands: Portrait of a pathological mantle plume. J. Geophys. Res. Solid
695 Earth 98, 19533–19563. https://doi.org/10.1029/93JB02018
696 Williams, C.D., Li, M., McNamara, A.K., Garnero, E.J., van Soest, M.C., 2015. Episodic
697 entrainment of deep primordial mantle material into ocean island basalts. Nat.
698 Commun. 6, 8937. https://doi.org/10.1038/ncomms9937
699 Workman, R.K., Hart, S.R., 2005. Major and trace element composition of the depleted
700 MORB mantle (DMM). Earth Planet. Sci. Lett. 231, 53–72.
701 https://doi.org/10.1016/j.epsl.2004.12.005
702 Zindler, A., Hart, S., 1986. Chemical Geodynamics. Annu. Rev. Earth Planet. Sci. 14, 493–
703 571. https://doi.org/10.1146/annurev.ea.14.050186.002425
704

This preprint has undergone one round of review in *Earth and Planetary Science Letters* and has been accepted for publication (as of April 2024)

Figures

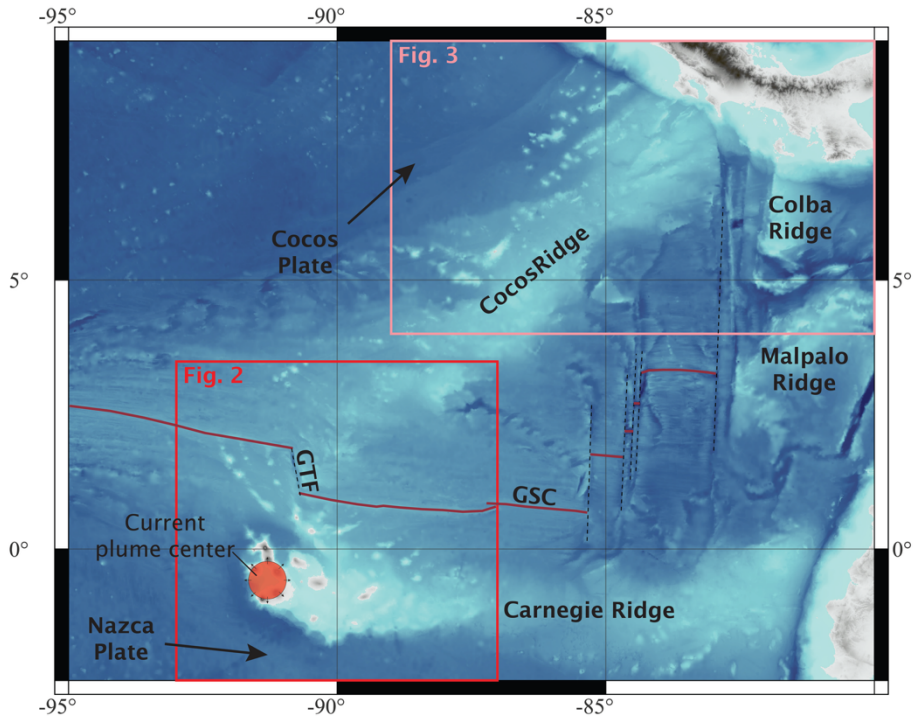

Figure 1 – *Overview map of the tectonic setting of the Galápagos Archipelago and Galápagos Spreading Center (GSC). The Galápagos mantle plume is currently located under the islands of Isabela and Fernandina in the western Galápagos, around 100-200 km south of the GSC. Volcanic activity driven by plume upwelling has generated the W-E Carnegie Ridge and the SW-NE Cocos Ridge on the Nazca and Cocos tectonic plates, respectively. Combined these ridges preserve a ~20 Myr record of plume related volcanism. The position of the Galápagos Transform Fault (GTF) separating the western and eastern GSC is also shown. Bathymetric data from GEBCO (General Bathymetric Chart of the Oceans). Figure generated in QGIS using the World Geodetic Survey (1984) Geographic Coordinate System with an equirectangular projection system*

710

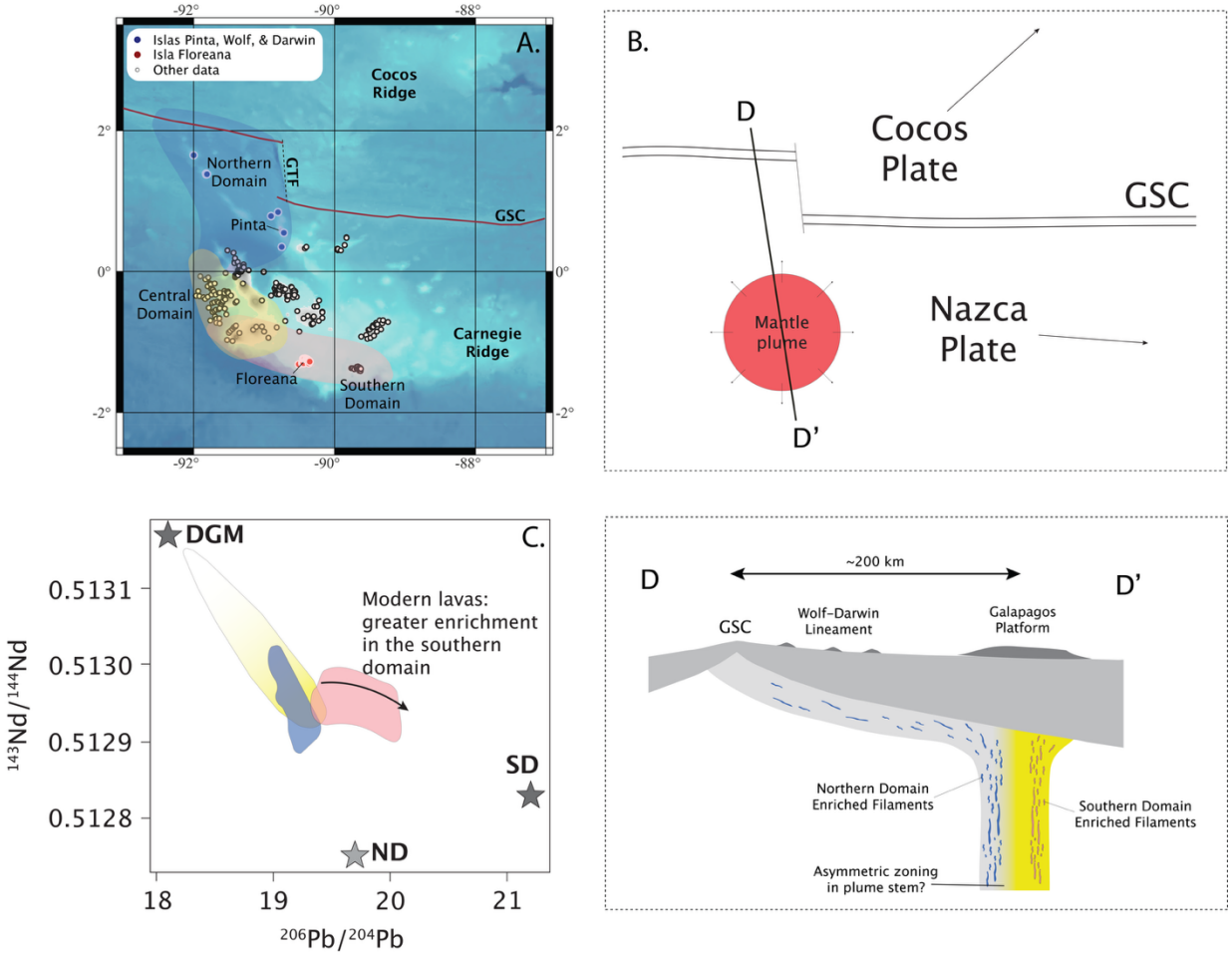

Figure 2 – *Tectonic setting and geochemical signatures of the Galápagos Archipelago.* ***A.*** *Lavas associated with the Galápagos plume show evidence for at least three spatially distinct enriched plume components. These are used to define the northern domain, central domain, and southern domain.* ***B.*** *Schematic representation of the current plume-ridge geometry, with the mantle plume located approximately 100-200 km south of the ridge axis.* ***C.*** *Fields representing the range of isotopic composition of basalts from the three domains, the data indicates a high degree of enrichment in basalts associated with the southern domain (Isla Floreana).* ***D.*** *Schematic cross section of the current plume-ridge geometry, with the ridge located to the north of the center of plume upwelling. This encourages flow of northern plume material towards the ridge and a greater mean depth of melting on the southern margin of the plume stem. The 'northern domain' plume component (**ND**) represents the new composition/end-member proposed in this study. The composition of the Southern Domain (**SD**) plume component and Depleted Galápagos Mantle (**DGM**) are taken from Harpp and White (2001).*

711

This preprint has undergone one round of review in *Earth and Planetary Science Letters* and has been accepted for publication (as of April 2024)

712

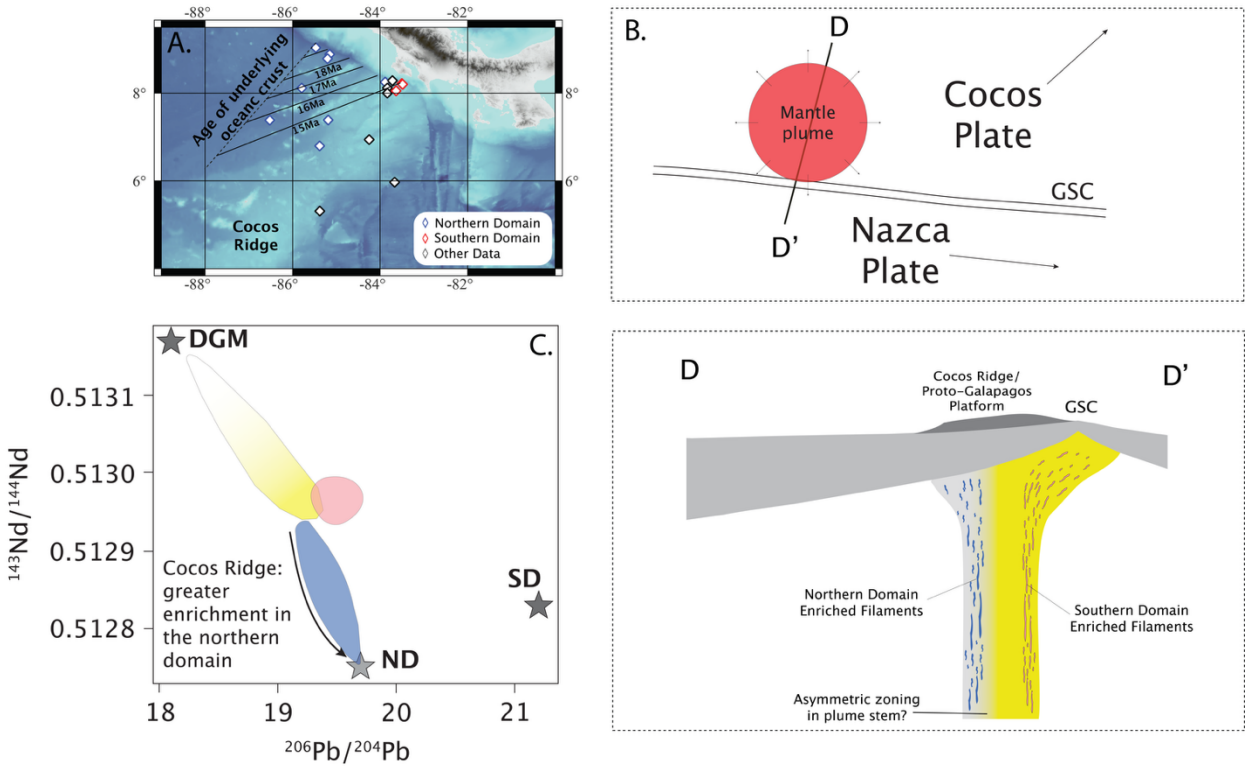

Figure 3 – *Tectonic setting and geochemical signatures of the northern Cocos Ridge (lava ages from 13 – 14.5 Ma).* ***A.*** *Erupted lavas in the northern Cocos Ridge display evidence for spatial zonation in plume composition, with distinct northern, central, and southern domains consistent with the geochemical enrichment in the modern-day Galápagos Archipelago (Hoernle et al. 2000). Plume related basalts of the northern Cocos Ridge are significantly younger than the underlying oceanic crust (Werner et al. 1999). Age of the underlying oceanic crust is taken from Barckhausen et al. (2001).* ***B.*** *Schematic representation of the plume-ridge geometry proposed by Werner et al. (2003) at ~12 – 14.5 Ma. The mantle plume is proposed to lie to the north of the ridge axis, with the southern margin of the plume potentially anchored on the ridge.* ***C.*** *Fields representing the range of isotopic composition of basalts from the northern Cocos Ridge that have been linked to the three enriched domains, the data indicates a high degree of enrichment in basalts associated with the northern domain.* ***D.*** *Schematic cross section of the plume-ridge geometry at ~12-14.5 Ma, with the ridge located to the south of the center of plume upwelling. This encourages flow of southern plume material towards the ridge and a greater mean depth of melting on the northern margin of the plume stem. The 'northern domain' plume component (**ND**) represents the new composition/end-member proposed in this study. The composition of the Southern Domain (**SD**) plume component and Depleted Galápagos Mantle (**DGM**) are taken from Harpp and White (2001).*

713

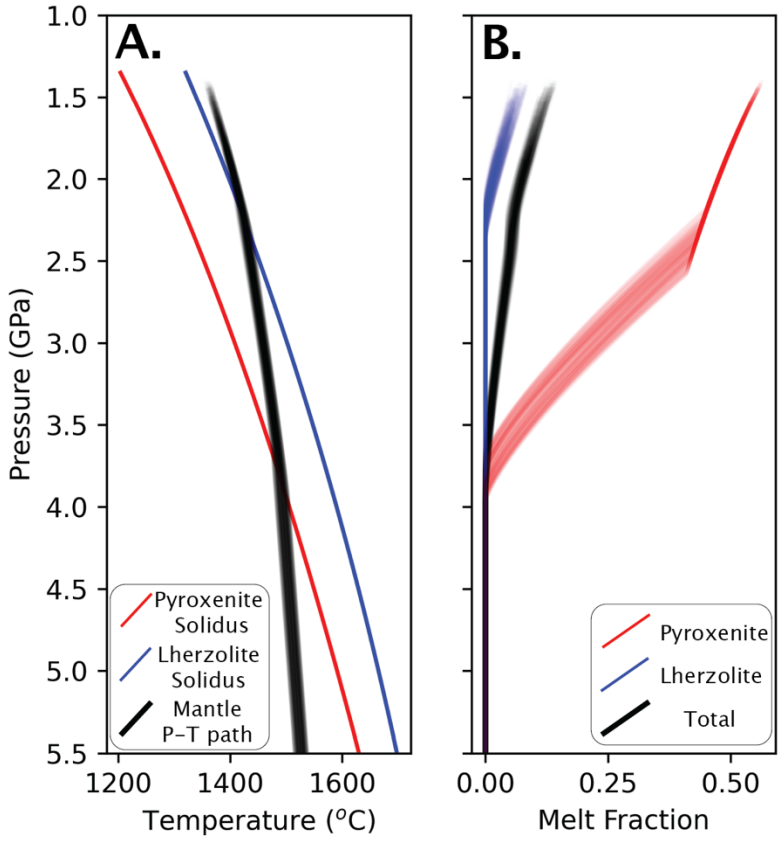

Figure 4 – *Pressure vs temperature (**A.**) and melt fraction (**B.**) for the mantle melting models used in this study. 200 models are shown with the mantle potential temperature set between 1400 and 1420 °C and the proportion of pyroxenite in the mantle source between 0.12 and 0.13.*

714
715

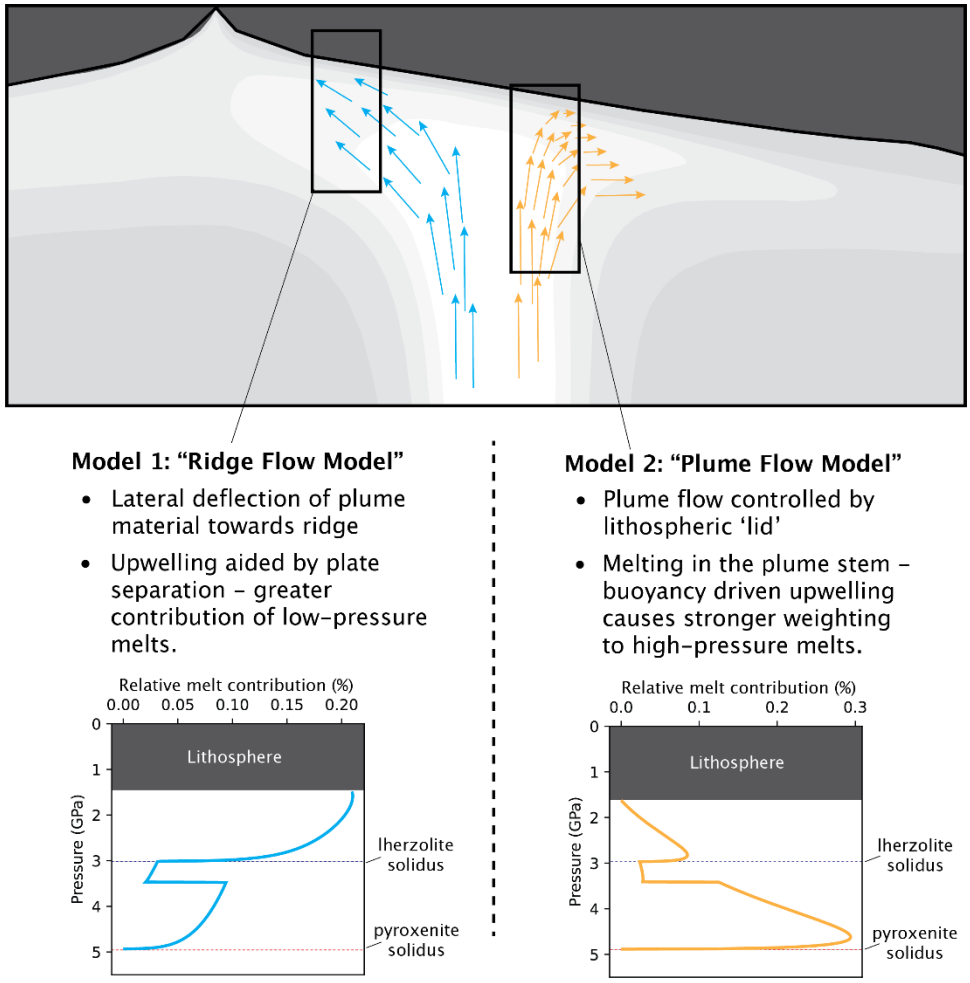

Figure 5 – *Schematic illustrations of the 2 different models considered in this study. Greyscale variations in the top diagram indicate temperature variations in the mantle with hotter temperatures indicated by lighter colors (adapted from Ito and Bianco, 2014). In Model 1, we assume plume material is flowing 'upslope' along the base of the mechanical lithosphere, with the upwelling velocity primarily controlled by passive upwelling during plate separation. This 'ridge flow' results in a relatively constant upwelling velocity across the melting region beneath the islands of Pinta, Wolf, and Darwin in the northern Galápagos. In Model 2, representing the far side of the mantle plume to off-ridge island formation, mantle upwelling rates are strongly pressure dependent as the upwelling, buoyant plume mantle upwells beneath the rigid lithospheric lid (with little 'upslope' flow towards a spreading center possible).*

716

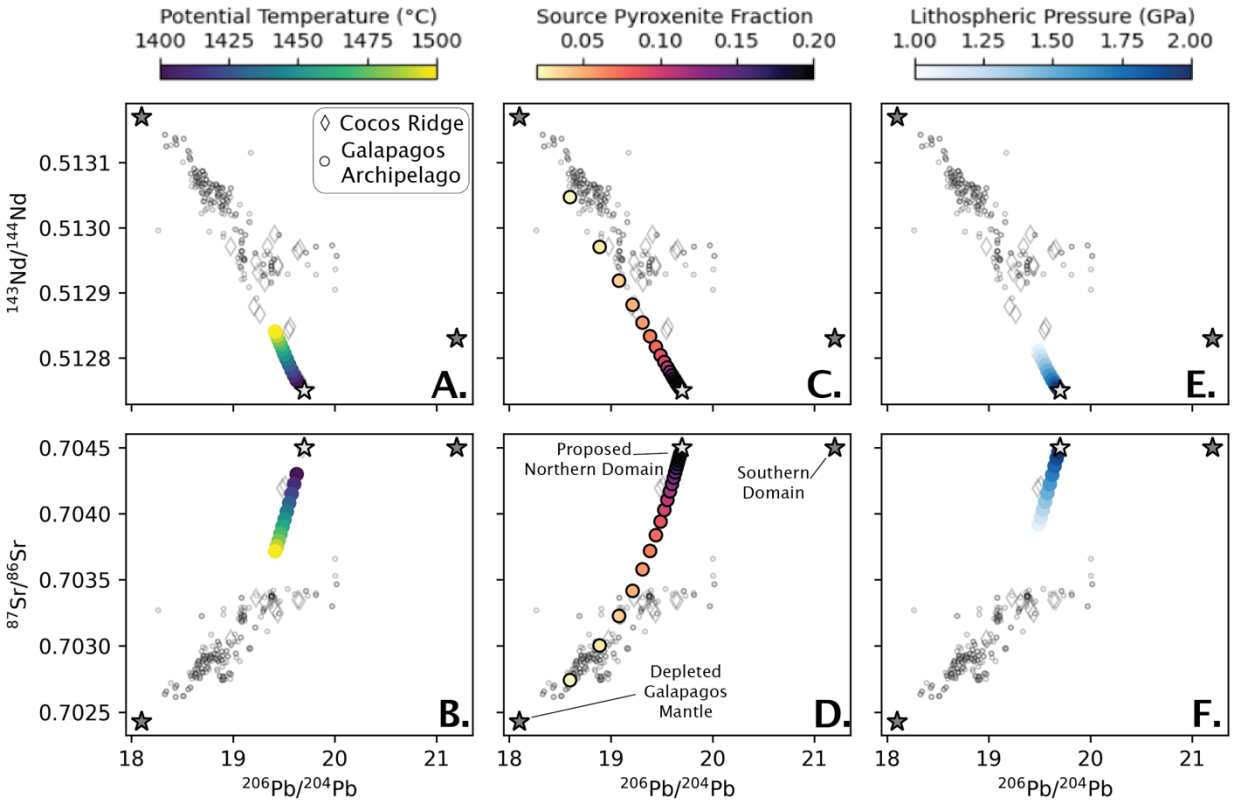

Figure 6 – *Isotopic composition of basalts from the Galápagos Archipelago and the Cocos Ridge against compositions predicted in Model 2 with individual parameters varying independently.* ***A. & B.*** *Influence of mantle potential temperature.* ***C. & D.*** *Influence of source pyroxenite fraction.* ***E. & F.*** *Influence of variations in lithospheric pressure. Geochemical data from the Galápagos Archipelago and Cocos Ridge taken from: (Allan and Simkin, 2000; Bow and Geist, 1992; Geist et al., 2005, 2002, 2006; Gibson et al., 2012; Gibson and Geist, 2010; Harpp et al., 2003; Harpp and Weis, 2020; Harpp and White, 2001; Hoernle et al., 2000; Kurz and Geist, 1999; McBirney and Williams, 1969; Naumann et al., 2002; Saal et al., 2007; Standish et al., 1998; Teasdale et al., 2005; White et al., 1993).*

717

718

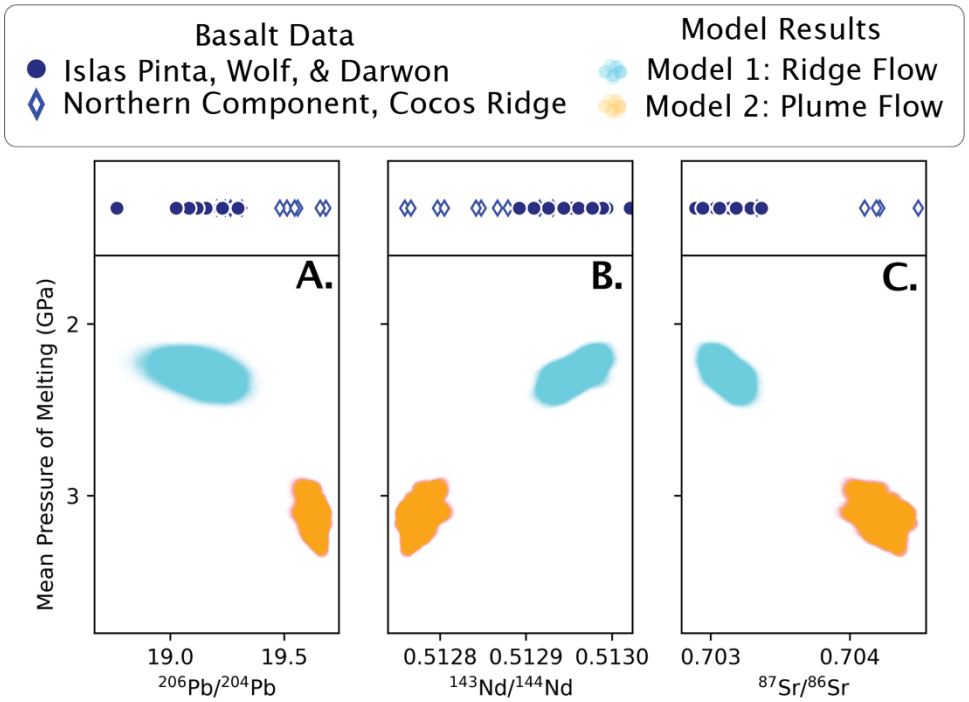

Figure 7 – *Isotopic compositions predicted for melting Models 1 & 2 for* ***A.*** *$^{206}Pb/^{204}Pb$,* ***B.*** *$^{143}Nd/^{144}Nd$, and* ***C.*** *$^{87}Sr/^{86}Sr$, with Model 2 simulations typically displaying more enriched signatures overlapping with the compositions observed in the northern domain of the Cocos Ridge.*

719

720

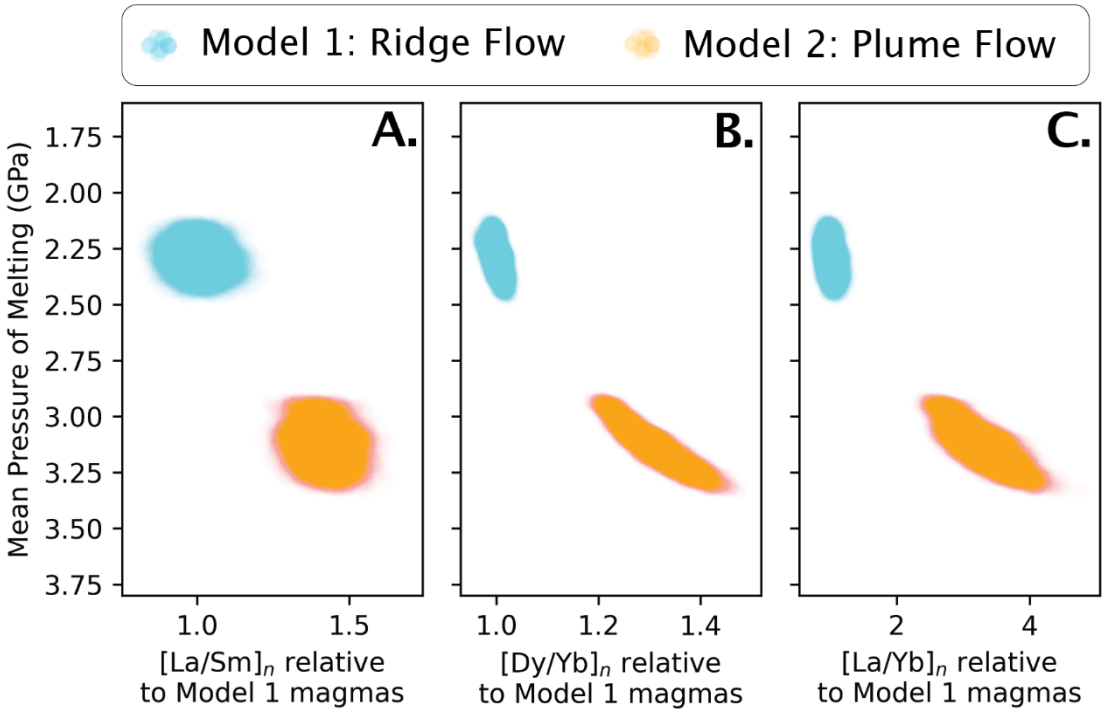

Figure 8 – *Trace element compositions predicted for melting Models 1 & 2.* ***A.*** *$[La/Sm]_n$ tracks the overall enrichment of the mantle sources and is sensitive to the mean melt fraction in each model (lower for Model 2).* ***B.*** *$[Dy/Yb]_n$ tracks the influence of garnet in the mantle residue and, therefore, is sensitive to the mean pressure of melting.* ***C.*** *$[La/Yb]_n$ represents a combination of the other two parameters. The subscript 'n' indicates normalization to the primitive mantle composition of Sun and McDonough (1989).*

721

722

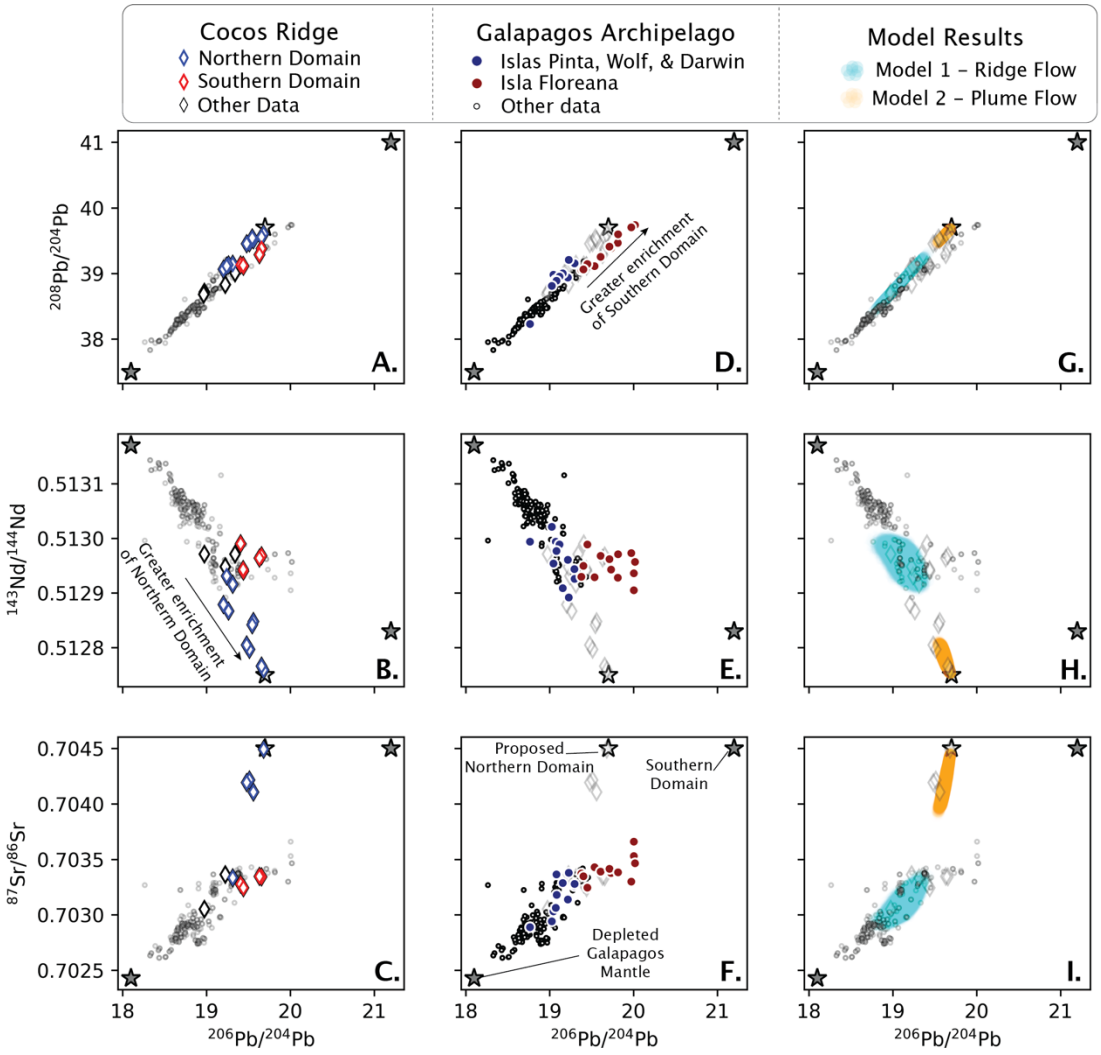

Figure 9 *– Isotopic compositions of basalts from the Cocos Ridge (**A. – C.**), the present-day Galápagos Archipelago (**D. – F.**), and magmas predicted by Model 1 & Model 2 mantle melting simulations (**G. – I.**). In all panels the composition of the Depleted Galápagos Mantle and southern ("FLO") component estimated by Harpp and White (2001) are indicated by the grey stars. The new composition proposed for the northern isotopic domain in the Galápagos mantle plume is also indicated by the lighter grey star in all panels. In panels **A. – C.** data from the Cocos Ridge displays a strong geochemical enrichment in basalts associated with the northern plume component. In contrast, panels **D. – F.** demonstrate that the strongest enrichment in the present-day Galápagos Archipelago is found in the southern isotopic domain (Isla Floreana). **G. – I.** Model 2 simulations produce more enriched isotopic compositions, overlapping with the enriched basalts collected along the northern margin of the Cocos Ridge (Hoernle et al. 2000).*

Supplementary Material: Persistent Geochemical Zonation ("Striping") within the Galápagos Mantle Plume

Matthew Gleeson[1]*, Mark Richards[1], Cinzia Farnetani[2], Kaj Hoernle[3], and Sally Gibson[4]

1. Melting behavior

Adiabatic decompression calculations are performed using the Python3 tool 'pyMelt' (Matthews et al. 2022) and parameterizations for the melting of the KLB-1 lherzolite and the KG1 pyroxenite from Matthews et al. (2021). Full details of the melting calculations and parameters used can be found in Matthews et al. (2021) and Katz et al. (2003), but are summarized briefly here.

Melting equations for both lithologies follow the form:

$$F = \begin{cases} T < T_{cpx-out}: \left(\dfrac{T - T_{solidus}}{T_{liquidus}^{lherz} - T_{solidus}}\right)^{\beta_1} \\ T > T_{cpx-out}: F_{cpx-out} + (1 - F_{cpx-out})\left(\dfrac{T - T_{cpx-out}}{T_{liquidus} - T_{cpx-out}}\right)^{\beta_2} \end{cases}$$

where:

$$T_{solidus} = A_1 \ln(P + A_2) + A_3 P + A_4$$

$$T_{liquidus} = B_1 \ln(P + B_2) + B_3 P + B_4$$

$$T_{liquidus}^{lherz} = C_1 \ln(P + C_2) + C_3 P + C_4$$

$T_{solidus}$ and $T_{liquidus}$ represent empirical parameterizations of experimental and/or thermodynamic predictions of the melting behaviour for each lithology. $T_{liquidus}^{lherz}$ is the theorectical temperature at which the system would be entirely molten if clinopyroxene-present melting continued beyond $F_{cpx-out}$, the melt fraction at which clinopyroxene is exhausted. $F_{cpx-out}$ is determined by:

$$F_{cpx-out} = \frac{M_{cpx}}{R_{cpx}(P)}$$

where:

$$R_{cpx}(P) = r_0 + r_1 P$$

2. Partition coefficients and source compositions

In this study we used trace element partition coefficients from Gibson and Geist (2010) and based our source compositions on prior estimates for the trace element content of the depleted MORB mantle (Workman and Hart, 2005) and subducted igneous crust (Stracke et al. 2003). The parameters used in our models are summarized in the tables below (Table S.1 & S.2):

Table S.1 – partition coefficients used in mantle melting models to perform trace element calculations

Element	Olivine	Clinopyroxene	Orthopyroxene	Garnet	Spinel
Pb	0.003	0.012	0.009	0.005	0.0
Sr	0.00004	0.091	0.0007	0.0007	0.0
La	0.0005	0.049	0.0031	0.001	0.01
Ce	0.0005	0.08	0.004	0.005	0.01
Pr	0.0008	0.126	0.0048	0.014	0.01
Nd	0.00042	0.178	0.012	0.052	0.01
Sm	0.0011	0.293	0.02	0.25	0.01
Eu	0.0016	0.335	0.013	0.496	0.01
Gd	0.0011	0.35	0.013	0.848	0.01
Tb	0.0015	0.403	0.019	1.477	0.01
Dy	0.0027	0.4	0.011	2.2	0.01
Ho	0.0016	0.427	0.0065	3.315	0.01
Er	0.013	0.42	0.045	4.4	0.01
Yb	0.02	0.4	0.08	6.6	0.01
Lu	0.02	0.376	0.12	7.1	0.01

Table S.2 – source trace element contents (all values reported in parts per million) used in this study.

Element	Depleted MORB Mantle (DMM) Workman and Hart (2005)	Subducted Igneous Crust (SIC) Stracke et al. (2003)	KG1 estimated composition (50:50 DMM:SIC excluding Sr & Pb)
Pb	0.018	0.09	0.18
Sr	7.664	81	26.824
La	0.192	1.68	0.926
Ce	0.55	5.89	3.220
Pr	0.107	n/a	n/a
Nd	0.581	7.45	4.0155
Sm	0.239	2.69	1.4645
Eu	0.096	1.04	0.568
Gd	0.358	4.03	2.194
Tb	0.07	n/a	n/a
Dy	0.505	5.01	2.7575
Ho	0.115	n/a	n/a
Er	0.348	3.13	1.739
Yb	0.365	2.99	1.678
Lu	0.058	0.45	0.254

3. Determining the relative melt contribution in Ridge Flow and Plume Flow models

Our study demonstrates that variations in the mean depth of melting can influence the composition of erupted basalts, without having to invoke changes in the source proportions. In the Galápagos variations in mean melting depth are controlled by differences in the plume dynamics in the melting region, resulting in an offset in the relative melt contribution from each pressure.

For Model 1 ("Ridge Flow") we assume a constant upwelling velocity of mantle through the melting region (primarily driven by passive upwelling in response to plate separation). Consequently, calculating the relative melt contribution from each depth/pressure interval to the final, homogenized melt composition is trivial:

$$w_{lith}^{P} = F\_inc_{lith}^{P} * X_{lith}$$

where w_{lith}^{P} represents the relative contribution of melts derived from lithology '$lith$' at pressure 'P'. Similarly, $F\_inc_{lith}^{P}$ is the incremental melt fraction of this lithology at the specified pressure and X_{lith} is the mass fraction of the specified lithology in the mantle source (prior to the initiation of melting). Importantly, w values are then normalized so that sum of the w values across each pressure interval and all different lithologies is equal to 1.

Constraining the depth- and lithology-dependent melt contribution factors is, however, more complex for the Model 2 ("Plume Flow") calculations. In this scenario there is a depth dependence to the upwelling velocity but, instead of calculating this directly, we chose to use the parameterization of Ito and Mahonney (2005) for the horizontal velocity of material leaving the melting region to determine the relative contribution of melts from each depth. The Ito and Mahonney (2005) parameterization states that the horizontal velocity of material leaving the melting region in a mantle plume setting is:

$$U(z) = 2\left(\frac{z}{H}\right) - \left(\frac{z}{H}\right)^2$$

Where z represents the depth of the region of interest (below the lithosphere) and H represents the maximum depth of the region of horizontal plume flow. By tracing the mantle components exiting the melting region at different depths we can calculate the depth-dependent melt contribution in regions away from the influence of a nearby spreading center. In this case we take H to also represent the base of the melting region to reduce the number of parameters that need to be fitted in our modelling. In addition, if the mantle has a constant average density across the melting region we can replace $\frac{z}{H}$ in the equation above with P', where $P' = \frac{P-P_{min}}{P_{max}-P_{min}}$ (P_{max} represents the max pressure of melting and P_{min} represents the pressure of melt termination).

$$U(P') = 2P' - P'^2$$

The relative melt contributions from each depth in the melting region can then be calculated:

$$w_{lith}^{P} = \sum_{0}^{P'} (U(P') * F\_inc_{lith}^{P} * X_{lith})$$

Ultimately this approach provides very similar depth-dependent melt contribution curves as assuming an exponential decrease in upwelling velocity of mantle material through the melting region with decreasing pressure (and 0 upwelling velocity at the base of the lithosphere).

4. Influence of the mixing parameter N

Incomplete homogenization and mixing of mantle melts from different lithologies and pressure intervals is simulated using a Dirichlet mixing function following the methods outlined by Rudge et al. (2013). We take this approach to try and simulate the natural variation in lava compositions associated with the northern domain of the Galápagos plume. The influence of varying the mixing parameter N is shown in Fig. S.1.

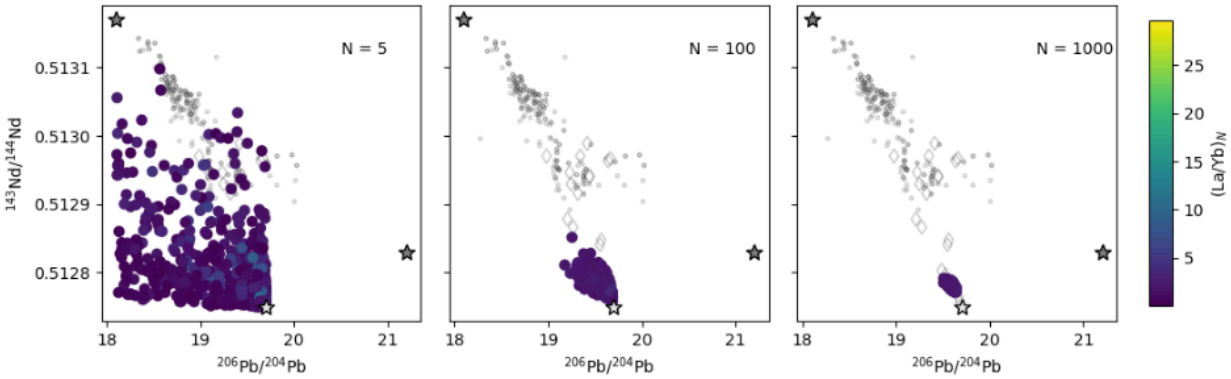

Fig S.1 *– Influence of varying the mixing parameter "N" on the composition of basalts sampled from the melting region. With increasing values of N the compositions converge on the 'true' average melt composition.*

References

Gibson, S.A., Geist, D.G., Day, J.A. and Dale, C.W., 2012. Short wavelength heterogeneity in the Galápagos plume: Evidence from compositionally diverse basalts on Isla Santiago. *Geochemistry, Geophysics, Geosystems*, *13*(9).

Ito, G. and Mahoney, J.J., 2005. Flow and melting of a heterogeneous mantle: 1. Method and importance to the geochemistry of ocean island and mid-ocean ridge basalts. *Earth and Planetary Science Letters*, *230*(1-2), pp.29-46.

Katz, R.F., Spiegelman, M. and Langmuir, C.H., 2003. A new parameterization of hydrous mantle melting. *Geochemistry, Geophysics, Geosystems*, *4*(9).

Matthews, S., Wong, K. and Gleeson, M., 2022. pyMelt: An extensible Python engine for mantle melting calculations. *Volcanica*, *5*(2), pp.469-475.

Matthews, S., Wong, K., Shorttle, O., Edmonds, M. and Maclennan, J., 2021. Do olivine crystallization temperatures faithfully record mantle temperature variability?. *Geochemistry, Geophysics, Geosystems*, *22*(4), p.e2020GC009157.

Rudge, J.F., Maclennan, J. and Stracke, A., 2013. The geochemical consequences of mixing melts from a heterogeneous mantle. *Geochimica et Cosmochimica Acta*, *114*, pp.112-143.

Stracke, A., Bizimis, M. and Salters, V.J., 2003. Recycling oceanic crust: Quantitative constraints. *Geochemistry, Geophysics, Geosystems*, *4*(3).

Workman, R.K. and Hart, S.R., 2005. Major and trace element composition of the depleted MORB mantle (DMM). *Earth and Planetary Science Letters*, *231*(1-2), pp.53-72.